



## Experimental Investigations of Static and Fatigue Crack Growth in Sandwich Structures with Foam Core and Fiber-Metal Laminates Face Sheets

F. Mazaheri, H. Hosseini-Toudeshky\*

Department of Aerospace Engineering, Amirkabir University of Technology, Tehran, Iran

**ABSTRACT:** Debonding of face-core interface is the most important damage mechanisms which make loss of structural integrity in sandwich structures. In this paper, mode-I and mode-II fracture of face-core interface in sandwich structures have been investigated under both static and fatigue loadings. The considered sandwich structures contain of different face sheet fiber-metal laminates and the core material is polyvinyl chloride foam. Several specimens are fabricated and the experiments are carried out to find the effects of initial debonding location and various fiber-metal laminate face sheets on the fracture toughness under static and fatigue loadings. Double cantilever beam specimens are used for mode-I and end notch flexure specimens for mode-II loading conditions. The resistance strength curves are plotted for mode-I and mode-II under static loading to find the instability point which is the border of stable and unstable crack growth and determine the critical crack length too. The strain energy release rates of mode-I and mode-II are also obtained for fatigue loading to investigate the resistance against damage evolution. Also, the global damage parameter is defined for both static and fatigue loading which is the combination of all damage mechanisms occurred in sandwich structures. Finally, the more efficient layup configurations under static and fatigue loadings among the investigated layups are introduced in mode-I and mode-II fracture conditions separately.

### Review History:

Received: 19 March 2018

Revised: 13 May 2018

Accepted: 24 June 2018

Available Online: 15 July 2018

### Keywords:

Sandwich structure

Fiber-metal laminate

Foam core

End notch flexure

Double cantilever beam

### 1- Introduction

Sandwich structures are widely used in many load bearing applications and they are increasingly employed in industries due to their high strength and stiffness and for weight reduction objective [1, 2]. Sandwich structures consist of two thin, stiff and high performance material face sheets adhesively bonded to a thicker lightweight core [3-5]. Additional advantages of using these structures are thermal and acoustic insulation, high energy absorption capabilities and integrated manufacturing. Fiber-Metal Laminates (FMLs) take the advantages of metal and fiber reinforced composites such as better damage tolerance to fatigue crack growth, ductility and impact damage with respect to composite face sheets specifically for aerospace applications [6-10]. Their structural attributes have led to the implementation of sandwich structures into many areas of industrial production and energy generation including aerospace, marine, automotive and wind turbine blades [11, 12]. But the application of sandwich structures in different engineering branch has been limited owing to the manufacturing process which may result in defects, damage and interfacial debonding between the face sheet and the core which make loss of structural integrity and catastrophic collapse of these structures [13, 14].

Delamination is an important failure mode in structural behavior of laminated materials which can decrease the stiffness and strength of material [15]. Delamination onset and growth is controlled by fracture toughness of the material. A variety of test methods have been developed to measure the face/core fracture toughness in sandwich structures, but none of the proposed methods have become an international standard to date [16]. One of the most popular test methods

proposed for determining the face/core fracture toughness under mode-I loading is the sandwich version of the Double Cantilever Beam (DCB) [17]. The End Notch Flexure (ENF) has been proposed to determine the fracture toughness under mode-II loading condition [18]. Besides, there are several studies that investigated the fracture toughness of sandwich structures under mixed-mode loading conditions [19, 20]. Fatigue failure mode of the sandwich structures is the important mode playing a major role in the final failure of sandwich components in many applications. Shenoj et al. [21] derived flexural fatigue characteristics of foam cored polymer composite sandwich beams with glass and aramid fibres skins set in epoxy resin and experiments were performed at different frequencies. Burman and Zenkert [22] investigated the fatigue response of sandwich structures with two cellular foam cores and the influence of the stress ratio was emphasized. It was seen that the fatigue behavior of the core materials is similar to classical metal fatigue. Kulkarni et al. [23] studied the fatigue crack growth of PolyVinyl Chloride (PVC) foam core sandwich beams under a three-point flexural loading. Fatigue data were collected for the S-N diagram and crack growth was monitored to develop a model for life prediction. Kanny and Mahfuz [24] studied the effects of frequency on the fatigue behavior of glass fiber reinforced sandwich composites with two different PVC cores. It was observed that the fatigue strength increased with core density and the crack growth rate decreased with increasing in the loading frequency. Bezazi et al. [25] analyzed the damage mechanisms of sandwich panels with PVC foam cores and fiber glass skins manufactured by vacuum molding and subjected to three-point bending fatigue tests. It was shown that the specimen with the larger core density withstands a larger load and possesses an enhanced fatigue resistance

Corresponding author, E-mail: hosseini@aut.ac.ir

compared to which with a lower core density. Zenkert and Burman [26] investigated the failure mode transition during constant amplitude loading fatigue tests of foam core sandwich beams. The obtained results demonstrated that for high load and small life cycle, the beams fail by core shear fracture while for lower load and large life cycle the beams fail by face sheet tensile failure. Yang et al. [27] studied fatigue damage of the sandwich structures consisting of aluminium skin sheets and foam core using three-point bending tests. The fatigue damage evolution started from the skin sheet fracture and then the foam core indentation was the failure mode.

There are little references about fatigue crack growth in a sandwich structure with an initial debonding. Burman and Zenkert [28] demonstrated the influence of initial damage in sandwich beams subjected to fatigue loading for the life prediction. The experimental measurement of interfacial fatigue crack growth rates in pre-cracked foam core sandwich beams has been carried out by Shipsha et al. [29]. The crack was propagated along the face sheet/core interface, in the core material, during fatigue loading and the crack growth was stable under constant amplitude testing. Also they [30] investigated mode-I fatigue crack propagation in foam core sandwich structures. The influence of various stress ratios and mean stresses on the fatigue crack growth rates was also examined. Static and cyclic debonding growth in PVC foam core sandwich specimens loaded in Mixed Mode Bending (MMB) was examined by Quispitupa et al. [31]. Static test were performed to determine the fracture toughness of the debonded sandwich specimens at different mixed mode loadings. The mixed mode ratio (mode I to mode II) was controlled by changing the lever arm distance of the MMB test rig. Fatigue results revealed higher deboned crack growth rates when the lever arm distance was increased. Manca et al. [32] studied the interface fatigue crack growth in pre-cracked foam core sandwich composites using the MMB test. The results revealed higher crack growth rates for mode I dominated loading and also different crack propagation paths observed for different foam cores and mode mixity ratios.

The aim of this paper is to investigate the delamination evolution of sandwich structures under static and fatigue loading regimes. The test set ups which have been followed in this work are DCB and ENF to simulate mode-I and mode-II fracture loading conditions. The novelty of this study is fabricating the sandwich structures with FML face sheets and PVC foam core thorough Vacuum Assisted Resin Transfer Molding (VARTM) method. This type of face sheets takes the advantages of both metal and fiber reinforced composites and the previous studies didn't consider this stacking

sequence, hence the static and low cycle fatigue behavior of these sandwich structures haven't been investigated yet. The comprehensive study has been performed in order to evaluate the debonding growth and progressive damage analysis in sandwich structures with different FML face sheets and initial debonding area under static and fatigue loading conditions. Finally, the more efficient layup configurations under static and fatigue loadings among the investigated layups are introduced in mode-I and mode-II fracture conditions separately.

## 2- Fabrication Process and Material Properties

In order to fabricate the sandwich structure with FML face sheets and PVC foam core, the FML face sheets were contracted using unidirectional E-glass fabric firstly and then bonded with the PVC foam core by the Epolam epoxy adhesive used for the fabrication of FMLs too (Fig. 1). To ensure that the adhesive thickness is uniform during the fabrication process, the samples are pressed with weights through the hand lay-up process for 24 hours till the complete curing. The material properties of PVC foam, epoxy adhesive, aluminum and E-glass/epoxy unidirectional lamina are presented in Tables 1 and 2. The initial debonding has been created by inserting Teflon film in between the layers during the manufacturing process. The initial debonding lengths are selected 50 (mm) and 30 (mm) for DCB and ENF specimens respectively. There are various methods to construct the FMLs such as placing the layup of metallic sheets and prepreg plies in a mold and exposing the structure to the elevated temperature and pressure in an autoclave. This manufacturing method results in well consolidated structures with perfect bonding between the metallic sheets and the fiber-reinforced composites. However, this fabrication process is expensive and the component size is limited by the size of autoclave [33].

Infusing liquid resin into dry fabric layers solely by vacuum pressure to produce high quality materials has proven to be a

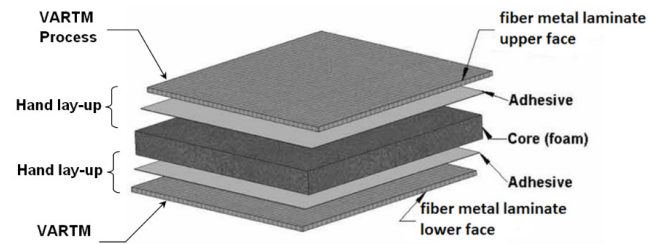


Fig. 1. Typical sandwich structure lay-up configuration

Table 1. Tensile material properties for aluminum [34] and epoxy (ASTM D638) and PVC foam (ASTM D638)

Samples	$E$ (GPa)	$E_T$ (GPa)	$\sigma_y$ (MPa)	$\sigma_u$ (MPa)	$\nu$
Epoxy	0.8625	0.6563	28.75	44.25	0.3
PVC Foam	0.1080	0.02	3.875	5.5	0.3
Aluminum 2024	73.1	-	324	-	0.33

Table 2. Material properties for glass/epoxy layers (ASTM D3039)

$E_{11}$ (GPa)	$E_{22}$ (GPa)	$E_{33}$ (GPa)	$G_{12}$ (GPa)	$G_{13}$ (GPa)	$G_{23}$ (GPa)	$\nu_{12}$	$\nu_{13}$	$\nu_{23}$
7	2.5	2.5	1.4	1.4	0.8	0.45	0.45	0.6

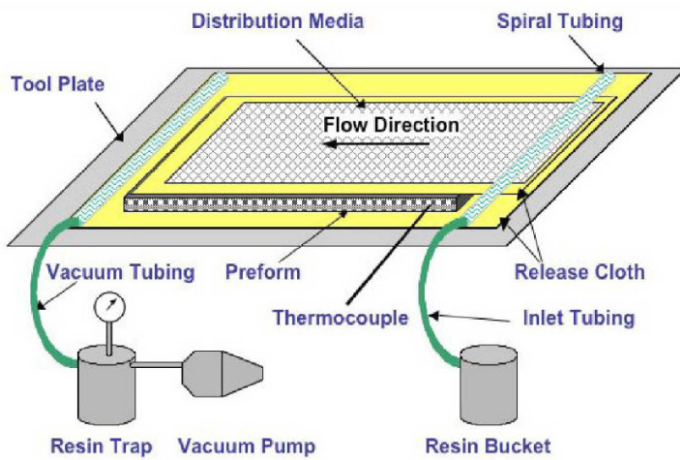


Fig. 2. VARTM process setup to construct FMLs face sheets

more cost effective process for preparing composites [35, 36]. This process known as VARTM, utilizes a flow distribution media to allow the resin to proceed rapidly on the surface over the length of the part followed by the slower infusion in the thickness direction of the laminate, thereby decreasing infusion times. Fig. 2 illustrates a typical VARTM set up used to fabricate the FMLs in this paper. This process makes high performance composite parts with high volume fractions without the use of an autoclave [37, 38].

Before fabricating of the FMLs, the surface treatments must be carried out to remove the aluminum oxide layer from the surface of aluminum substrates for appropriate bonding with composite laminates and PVC foam. There are several treatment methods for the preparation of metal surfaces such as: mechanical, chemical, electrochemical, coupling agent and dry surface treatments [7]. We chose the chemical surface treatment based on P2 etching procedure. The surface treatment procedure was based on the following steps [39, 40]:

1. Cleaning aluminums with acetone.
2. Immersing them in alkaline solution and then rinsed in tap water.
3. Immersing them in an aqueous acidic solution containing Fe(III) and sulfuric acid in enough water and then rinsing the specimens in deionized water and drying the aluminums in an oven.

### 3- Static Tests Setup

The main advantage of sandwich structures is that they are stiff and light, but they have to be strong as well. There are at least 5 different modes of failure for the composite sandwiches when loaded in bending [41]; a given structure may fail at which ever mode occurs at the lowest load. Based on Fig. 3, the failure modes are; (a) yielding or fracture of the tensile face, (b) buckling or wrinkling of the compression face, (c) failure of the core in shear all though there is also a lesser possibility of tensile or compressive failure of the core, (d) the possibility of indentation of the faces and core at the loading points and (e) the failure of the bond between the

faces and core that is so-called debonding which is the most important and complex failure mechanism for the analyses. This failure mechanism can be characterized by fracture toughness test like methods.

While there is no ASTM standard for sandwich structure fracture toughness calculations under static loading, the procedure of the tests and specimen dimensions followed the standard ASTM D5528 for DCB specimens and ASTM D6671 for ENF specimens to measure the face/core delamination fracture toughness (ASTM WK22949 for determination of the Mode II is in preparation). The sandwich beams investigated for DCB and ENF tests contain of three layups of (Al//Foam/Al), (Al/90/0//Foam/0/90/Al), and (Al//90/0//Foam/0/90/Al) which denotes an initial crack or debonding at the face/core interface. To achieve the quasi static condition in a displacement control mode, all tests have been performed at a crosshead speed of 1 (mm/min)) using a 50 kN servo hydraulic test apparatus and each type of experiment has been repeated for three times. All tests specimens are already pre-cracked and for static debonding growth the crack lengths are measured and recorded using a travelling microscope [16].

Fig. 4 indicates the servo hydraulic test apparatus and corresponding specimens during DCB and ENF tests. For the DCB test shown in Fig. 4 (a) the load is applied perpendicular to the initial crack direction to create tensile stresses on the adhesive interface and the specimens were connected to the test rig by piano hinges, for ENF tests illustrated in Fig. 4 (b) the specimens are subjected to three points bending condition in a fixture with rounded loading point to create pure shear stress at the mid-thickness of the foam. Fracture toughness has been evaluated in terms of mode-I critical energy release rate  $G_{IC}$  given by [43]:

$$G_{IC} = \frac{A}{\Delta a \times W} \quad (1)$$

where,  $W$  is the specimen width (mm),  $\Delta a$  is the propagated debonding length (mm), and  $A$  is the energy (N.mm) to achieve the total propagated debonding length in Fig. 5 (a).

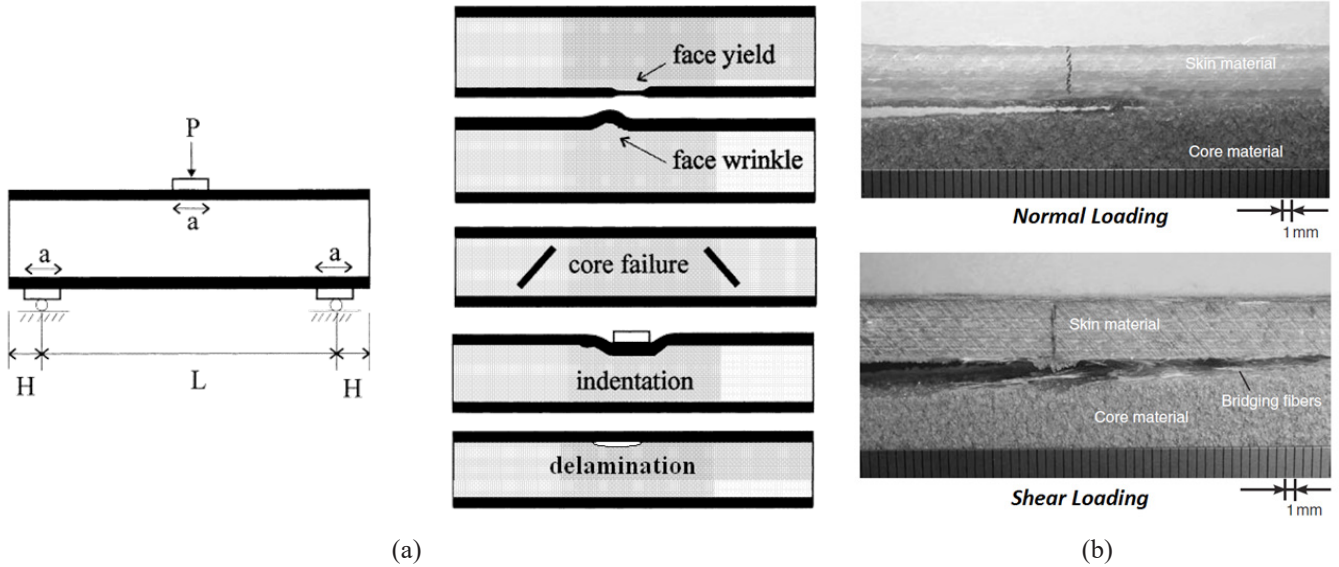


Fig. 3. Damage mechanisms in a sandwich structure; (a) different damage modes, (b) specimens under mode-I and mode-II fracture [42]

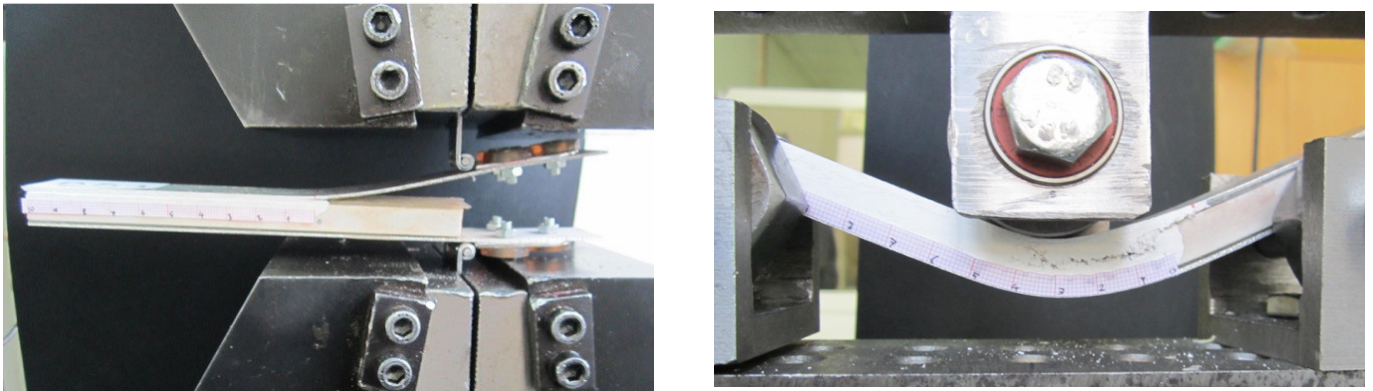


Fig. 4. Specimens under load; (a) DCB test, (b) ENF test

Mode-II interlaminar fracture toughness is calculated from the initial debonding length and the load-deflection curve using the highest load and deflection level using Direct Beam Theory (DBT) [44]:

$$G_{IIc} = \frac{9P\delta a_0^2}{2W(0.25L^3 + 3a_0^3)} \quad (2)$$

where,  $P$  is the load (N),  $\delta$  is the displacement (mm),  $W$  is the specimen width (mm),  $L$  is the specimen span (mm) and  $a_0$  is the initial debonding length (mm) as seen in Fig. 5 (b).

To predict the behavior of sandwich structures under static loading, the global damage parameter can be defined which depends on the stiffness reduction of specimen. The global damage is the combination of all damage mechanisms in the unique parameter and given by:

$$D = 1 - \frac{\text{Stiffness}}{\text{Maximum Stiffness}} = 1 - \frac{P\delta_{cr}}{P_{cr}\delta} \quad (3)$$

where,  $P_{cr}$  is the maximum load (N),  $\delta_{cr}$  is the displacement (mm) corresponding to maximum load.

#### 4- Results and Discussion of Static Tests

The obtained load–displacement curves from mode-I and mode-II experiments are shown in Figs. 6 (a) and 7 (a). The maximum load value achieved for each group of specimens gives a qualitative view of the interface joint strength and represents the specific load that the crack initiation is occurred. Fig. 6 (b) demonstrates when the displacement reaches 43 (mm), the delamination growth of (Al//90/0/Foam/0/90/Al) sandwich layup is greater than (Al//Foam/Al) and (Al/90/0//Foam/0/90/Al) layups. In (Al/90/0//Foam/0/90/Al) sandwich beams debonding propagates in PVC foam core because foam strength is weaker than the interface strength.

Global damage parameter for different layup configurations under mode-I static loading is derived in Table 3. This table shows that (Al//foam/Al) sandwich layup has the smallest damage growth and it has no damage until the displacement value of 35 mm. But considerable damage propagations are existed in (Al//90/0/Foam/0/90/Al) layup configuration and at the displacement of 65 mm global damage parameter reaches unit value and the layup is almost destroyed.

Fig. 7 (b) indicates that the debonding growth of (Al//Foam/Al) sandwich layup is almost smaller than (Al//90/0/Foam/0/90/Al) and (Al/90/0//Foam/0/90/Al) layups

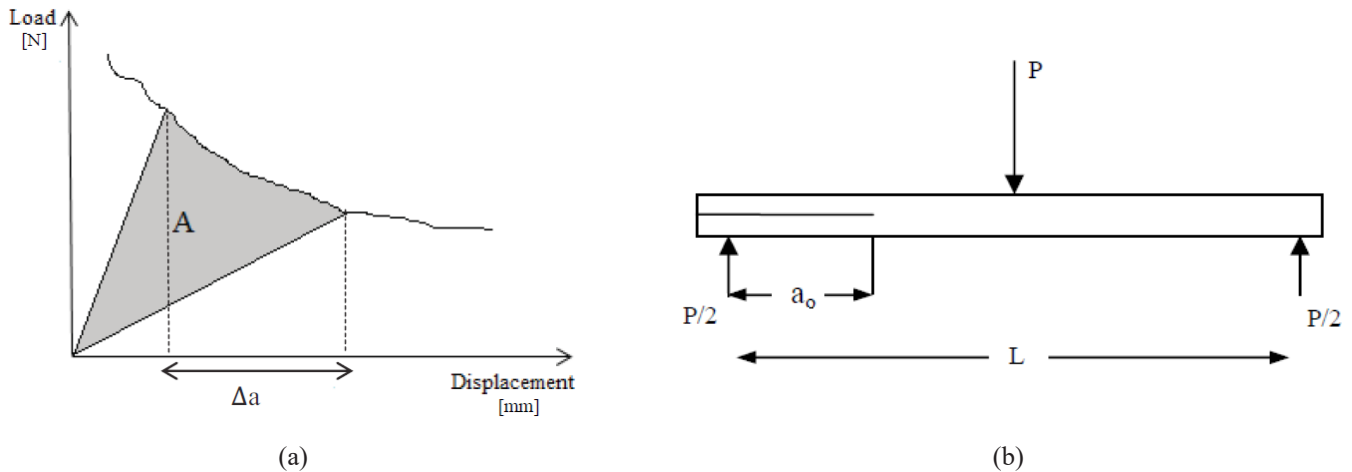
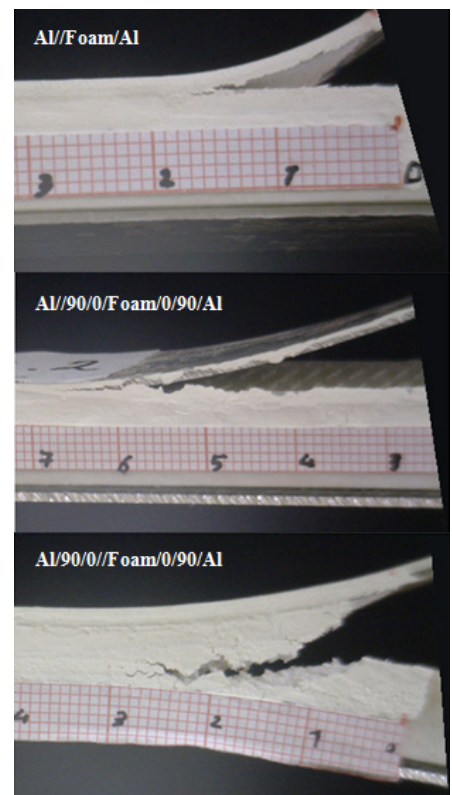
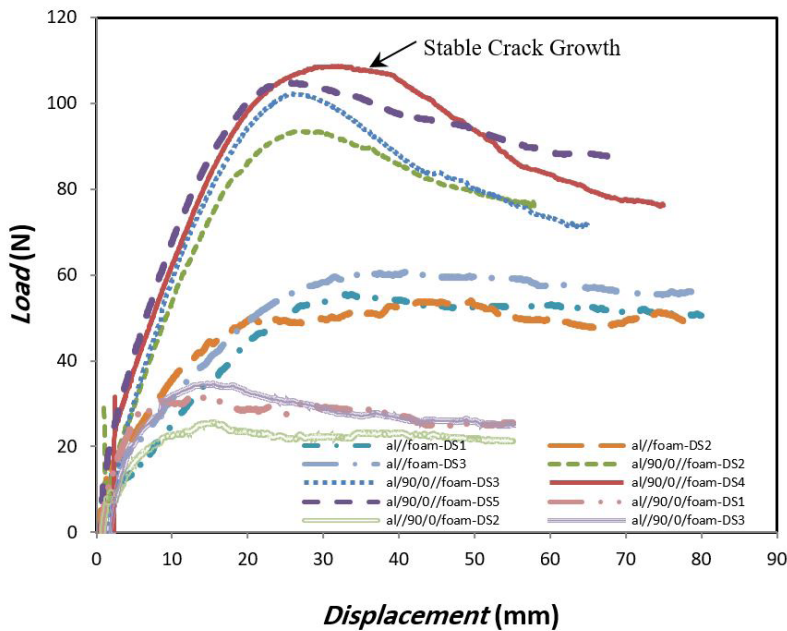


Fig. 5. Schematic presentation of (a) fracture energy A determination, (b) ENF Specimen



(a) (b)

Fig. 6. Mode-I (a) load-displacement curve, (b) debonding and crack growth at 43(mm) displacement.

when the displacement value reaches 25 mm. In mode-II loading condition, shear force is large enough to initiate and propagate crack in the PVC foam core of (Al//90/0//Foam/0/90/Al) layup configurations instead of delamination growth between aluminum and composite. Also, in mode-II displacement controlled tests, the crack has deviated and the same displacement value is observed again until the structure suffers a catastrophic failure or the crack again behaves in a stable manner. In other words, unstable crack growth is presented when the load–displacement curve has a semi-vertical tangent. In all other test results in mode-I and mode-II, stable crack growths are occurred [45]. Table 4 depicts the global damage parameter in mode-II static loading. We can

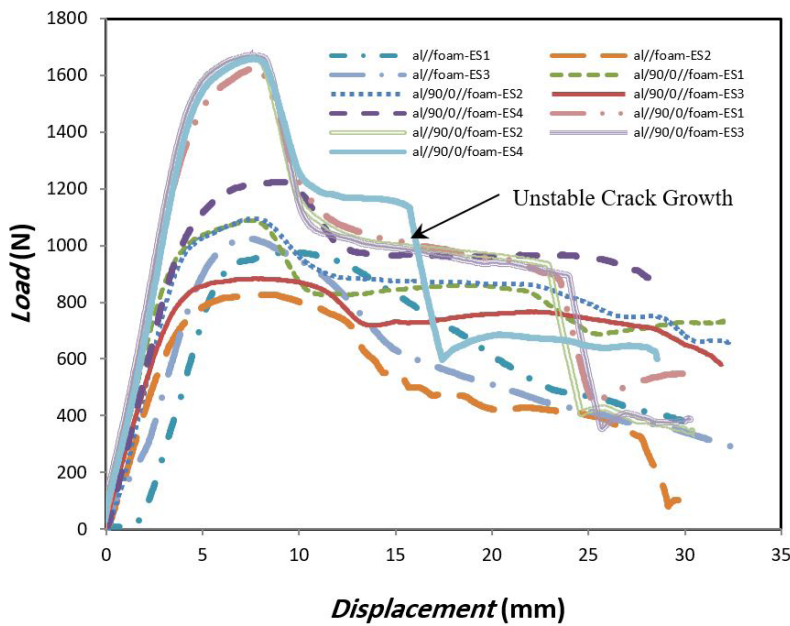
realize that the (Al//foam/Al) sandwich layup fails before the other layups when the displacement value reaches 30 mm. Generally, it can be noted that the level of loading value to initiate the debonding growth in mode-II is larger than mode-I and, the debonding and crack growth of mode-II static loading is faster than mode-I with assuming the same crosshead speed of 1 (mm/min). The mean experimental values of fracture toughness for mode-I and mode-II are listed in Table 5. In mode-I tests, the results show the interface strength between the aluminum and composite in (Al//90/0//Foam/0/90/Al) is weaker than the other layups interfaces since it has the minimum load corresponding to the point which damage occurs.

**Table 3. Global damage parameter for mode-I static loading.**

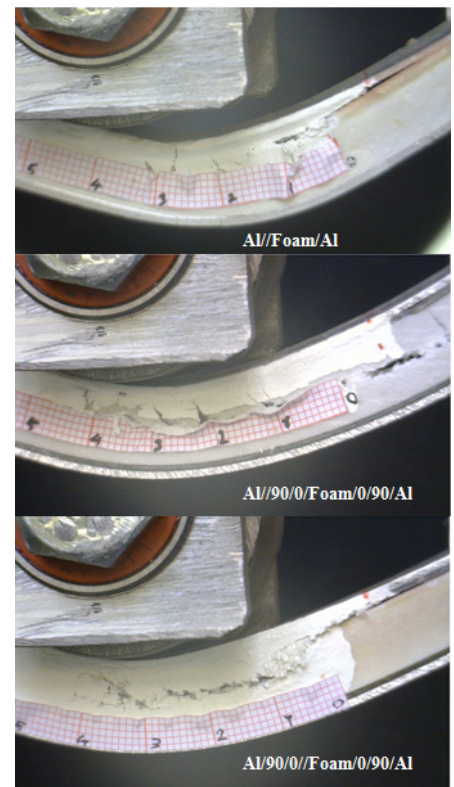
Displacement (mm)	Global Damage Parameter		
	Al/90/0//Foam/0/90/Al	Al//Foam/Al	Al//90/0//Foam/0/90/Al
35	0.3295	0.0092	0.6940
40	0.4530	0.1302	0.7409
45	0.5395	0.2322	0.7750
50	0.6016	0.3141	0.7998
55	0.6527	0.3815	0.8267
60	0.6978	0.4405	0.8937
65	0.7247	0.4932	1.0894

**Table 4. Global damage parameter for mode-II static loading.**

Displacement (mm)	Global Damage Parameter		
	Al/90/0//Foam/0/90/Al	Al//Foam/Al	Al//90/0//Foam/0/90/Al
10	0.1376	0.1790	0.4052
15	0.5248	0.6288	0.6778
20	0.6418	0.7822	0.8559
25	0.7150	0.8372	0.8730
30	0.8153	1.0162	0.7608



(a)



(b)

**Fig. 7. Mode-II (a) load-displacement curve, (b) debonding and crack growth at 25 (mm) displacement.**

The fracture resistance of  $G_{IR}$  and  $G_{IIR}$  as a function of debonding length were determined for DCB specimen for mode-I and ENF specimen for mode-II respectively. During debonding growth, the multiple damage mechanisms such as foam core failure and matrix cracking and other damages

occur which increase the apparent fracture toughness of the interface (especially in mode-II). Therefore, it is suggested that  $G_R$  (a) is determined from a quasi-static test which could presents a better phenomenological parameter as it combines many different damage effects that change resistance into

**Table 5. Obtained fracture toughness values for DCB and ENF tests**

Samples	$G_{IC}$ (N/mm)	$G_{IIC}$ (N/mm)	Considerations
Al/Foam/Al	1.4768	1.3544	-
Al/90/0//Foam/0/90/Al	2.0136	1.5640	-
Al//90/0/Foam/0/90/Al	0.3206	2.1459	Only crack growth in the middle of foam thickness in ENF tests.

one value in R-curve. Unlike fracture toughness  $G_C$ , the  $G_R$  (a) curve is specific as it depends on the material, stacking sequence, and other forms of involved mechanisms [46]. The use of the R-curve implies that the quasi-static delamination mechanism is the same as the fatigue delamination mechanism and therefore the resistance to quasi-static growth also determines the resistance to fatigue growth.

The obtained R-curves from mode-I and mode-II experiments are shown in Figs. 8 and 9 respectively. Three conditions may be occurred: the fracture resistance is greater than the driving force (stable crack growth  $G_R(a) < G_C$ ), the fracture resistance is equal to the driving force (instability point  $G_R(a) = G_C$ ) and the driving force is greater than the fracture

resistance (unstable crack growth  $G_R(a) > G_C$ ). Fig. 8 demonstrates that in mode-I loading all sandwich layups have stable crack growth when we increase the crosshead displacement until  $G_{IR}(a) < G_{IC}$ , if  $G_{IR}(a)$  reaches  $G_{IC}$  value, the damage propagation will shift to unstable crack growth till to catastrophic failure. Also, we found that from Fig. 8 (d), the debonding growth of (Al//90/0/Foam/0/90/Al) sandwich layup is more unstable than those in (Al//Foam/Al) and (Al/90/0//Foam/0/90/Al) layups because it has the maximum crack growth with the minimum driving force. In mode-I static loading the (Al//90/0/Foam/0/90/Al) sandwich layup has the smallest resistance against the debonding growth, so it is the least efficient layup configuration.

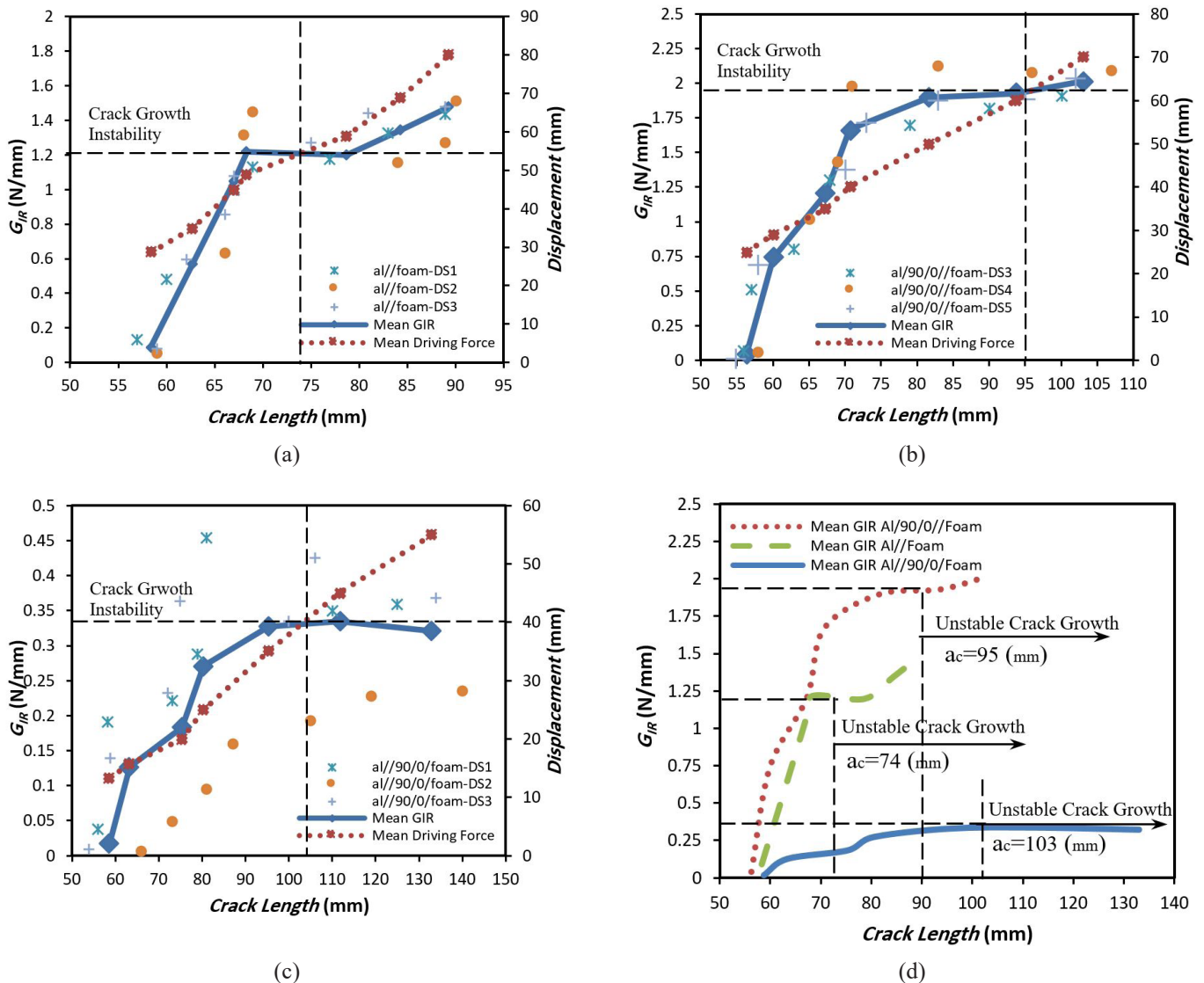


**Fig. 8. R-curves for DCB Specimens (a) Al//Foam/Al, (b) Al/90/0//Foam/0/90/Al, (c) Al//90/0/Foam/0/90/Al, (d) Mean value of different lay-ups**

It should be noted that measuring the crack length in mode-II is very complex as due to the existed shear stresses the foam cracks are inclined with respect to the initial debonding. For example, for (Al//90/0/Foam/0/90/Al) layup configurations, this stress is large enough to damage the whole foam core without any initial debonding growth. This could be a major reason for larger scattering of the results in mode-II with respect to mode-I tests results. Fig. 9 indicates that in mode-II loading all sandwich layups have unstable crack growths since the beginning of loading (especially above 25 (mm) driving force) the fracture resistance  $G_{IIR}$  (a) is greater than fracture toughness  $G_{IIc}$ . As we increase the crosshead displacement for (Al//90/0//Foam/0/90/Al) specimens, the slope of R-curve tends to infinity because there are no arrested cracks and whole energy is dissipated to create new cracks and coalesce them or transform failure mode from debonding growth to damage in composite. So, in mode-II static loading, the (Al//Foam/Al) sandwich layup has the most predictable manner.

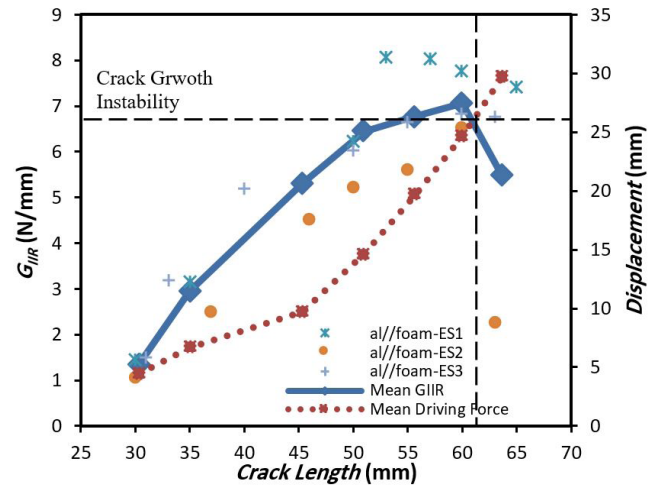
### 5- Fatigue Tests Setup

Debonding is a major weakness of sandwich structures and understanding the resistance of these structures to interlaminar fracture under fatigue loading is essential for making guidelines for allowable and damage tolerance design. All DCB and ENF fatigue tests were conducted under constant amplitude displacement control at a load frequency of 0.5 Hz with displacement ratio of  $R = \delta_{min} / \delta_{max} = 0.05$  using the same test apparatus and fixtures employed for static tests (Fig. 4). Also the same setup and three of DCB and ENF specimen layup configurations that were used for static tests were also used in the fatigue tests. Similar to static tests, all test specimens were already pre-cracked and for fatigue debonding growth the delamination lengths were measured and recorded by travelling microscope. The procedure of the tests and specimen dimensions followed the standard ASTM D6115 for DCB specimens. Based on this standard, the delamination growth was generated by applying  $\delta_{max} = \sqrt{0.5}[\delta_{cr-av}]$  which  $[\delta_{cr-av}]$  is the average value of the critical load point displacement for delamination growth at the end of the insert in a quasi-static test. The maximum cyclic mode-I strain energy release rate,  $G_{I_{max}}$  is calculated by Beam Theory (BT) [47]:

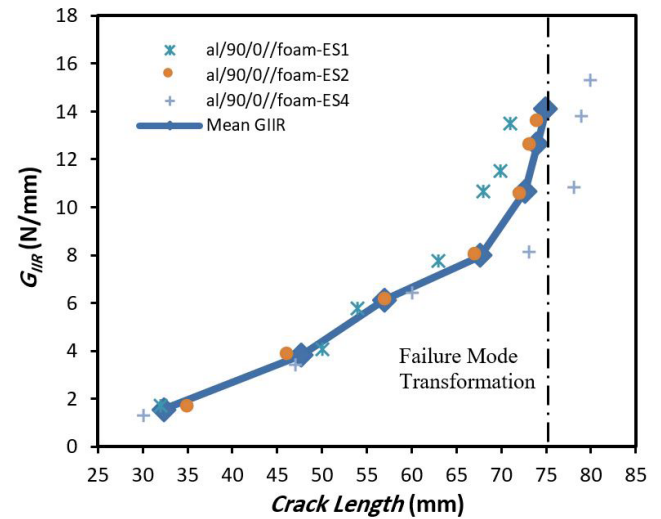
$$G_{I_{max}} = \frac{3P_{max} \delta_{max}}{2Wa} \quad (4)$$

where,  $\delta_{max}$  and  $P_{max}$  are maximum cyclic displacement (mm) and load (N) respectively. Also,  $a$  is debonding length (mm). Recently the ENF test is also used for measuring the behavior of mode-II interlaminar delamination under fatigue loading. But until now no standard has been developed for mode-II delamination under fatigue loading. Hence we followed the ASTM D6115 for loading conditions and ASTM 6671 for specimen dimensions (according to Fig. 5 (b)) and determination of maximum cyclic mode-II strain energy release rate  $G_{II_{max}}$  by Direct Beam Theory (DBT) [48]:

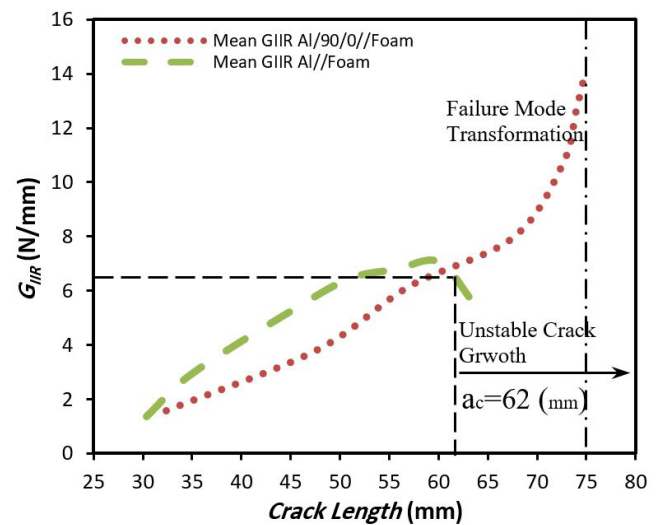
$$G_{II_{max}} = \frac{9P_{max} \delta_{max} a^2}{2W (0.25L^3 + 3a^3)} \quad (5)$$



(a)



(b)



(c)

Fig. 9. R-curves for ENF Specimens (a) Al//Foam/Al, (b) Al/90/0//Foam/0/90/Al, (c) Mean value of different layups

During the fatigue tests, decreasing in load according to the number of cycles was recorded. In displacement control tests, the load reduction  $F_{max}/F_{0max}$  is equivalent to stiffness reduction. This ratio is reported as a function of cycles number and it is related to the decrease of fatigue modulus. The experimental results showed that the load reduction can be expressed as a logarithmic function of fatigue cycles as [49]:

$$\frac{F_{max}}{F_{0max}} = A_{0d} - A_d \ln(N) \tag{6}$$

where,  $N$  is cycles number,  $A_{0d}$  depends on the initial conditions (which is equal to  $F_{max}$  at  $N=1$ ) and  $A_d$  depends on the applied displacement value and the material properties. The fatigue behavior of the sandwich composites mainly depends on the progressive developments of damage mechanisms such as matrix cracking, delamination, and fiber breakage in the skins and interfacial debonding between core and skin and shear cracks in the core. We combine all damage mechanisms in a global damage parameter  $D$ , which depends on the type of reinforcement, core characteristics, maximum applied loading level and type of loading as [49]:

$$D = \frac{F_{0max}}{F_{max}} [A_d \ln(N)] \tag{7}$$

**6- Results and Discussion**

In displacement control fatigue tests, the delamination growth in initial cycles is faster than final cycles. The damage accumulates faster at low number of cycles and it propagates gradually at higher number of cycles. Figs. 10 (a) and 10 (b) illustrate the delamination growth and maximum cyclic strain energy release rate in mode-I loading condition against number of cycles. From these figure we can understand that if the number of cycles increases, the  $G_{Imax}$  will decrease too. At initial number of cycles when  $G_{Imax} > G_{IC}$  the fatigue debonding growth is very fast, with increasing the number of cycles,  $G_{Imax}$  is equal or less than mode-I delamination fracture toughness, hence the fatigue debonding growth rate reduces and debonding or crack will remain unchanged near the failure cycles. As mentioned before, under mode-I static loading the

critical load point displacement for delamination growth in (Al/90/0/Foam/0/90/Al) layup is about half of the other layups. Since  $\delta_{max} = \sqrt{0.5}[\delta_{cr}]_{av}$ , the maximum displacement of this configuration under mode-I fatigue loading is about half of the other layups. Thus the fatigue debonding growth of (Al/90/0/Foam/0/90/Al) sandwich layup is smaller than (Al//Foam/Al) and (Al/90/0//Foam/0/90/Al) layup configurations. Figs. 10 (c) and 10 (d) illustrate the load reduction and damage evolution versus the number of cycles for several sandwich layups in mode-I loading condition respectively. In displacement control DCB fatigue tests, the (Al/90/0//Foam/0/90/Al) sandwich layup has the more stiffness reduction with respect to the other layup configurations, subsequently damage growth of (Al/90/0//Foam/0/90/Al) layup is faster than those obtained for (Al//Foam/Al) and (Al/90/0//Foam/0/90/Al) layups. Since the maximum displacement of (Al/90/0//Foam/0/90/Al) configuration under mode-I fatigue loading is smaller than the other layups, Hence the damage evolution of this sandwich layup is smaller than the other layup configurations. After 3000 cycles, the total debonding or crack length for (Al/90/0//Foam/0/90/Al) layup configurations is about 30 mm and it is greater than those for (Al//Foam/Al) and (Al/90/0//Foam/0/90/Al) sandwich layups (Fig. 11). If we consider two layups with the same maximum displacement, the (Al//Foam/Al) sandwich layup has greater resistance against the debonding growth with respect to (Al/90/0//Foam/0/90/Al) layup and it is more efficient layup configuration. It is predictable, since similar to static loading the debonding propagates in PVC foam core of (Al/90/0//Foam/0/90/Al) sandwich beam whose strength is weaker than the interface strength. The global damage parameter for different sandwich beams under mode-I fatigue loading are gathered in Table 6. According to this table, (Al/90/0//Foam/0/90/Al) sandwich beam is the first layup configurations whose global damage parameter reaches unit about 1000 cycles and it has the greatest damage growth rate versus the number of cycles.

It should be mentioned that the maximum displacement of all specimens under mode-II fatigue loading is equal. Similar to static loading, we observed that foam core shear failure occurred instead of initial debonding growth in (Al/90/0//Foam/0/90/Al) sandwich layup. Figs. 12 (a) and 12 (b) illustrate the delamination growth and maximum cyclic strain energy release rate in mode-II loading condition against the

**Table 6. Global damage parameter for mode-I fatigue loading.**

Number of Cycles	Global Damage Parameter		
	Al/90/0//Foam/0/90/Al	Al//Foam/Al	Al/90/0//Foam/0/90/Al
100	0.4520	0.5534	0.4886
200	0.5746	0.6254	0.5611
300	0.6612	0.6718	0.6083
400	0.7304	0.7068	0.6442
500	0.7891	0.7352	0.6735
600	0.8405	0.7593	0.6984
700	0.8866	0.7802	0.7202
800	0.9285	0.7989	0.7397
900	0.9672	0.8156	0.7573
1000	1.0031	0.8310	0.7733

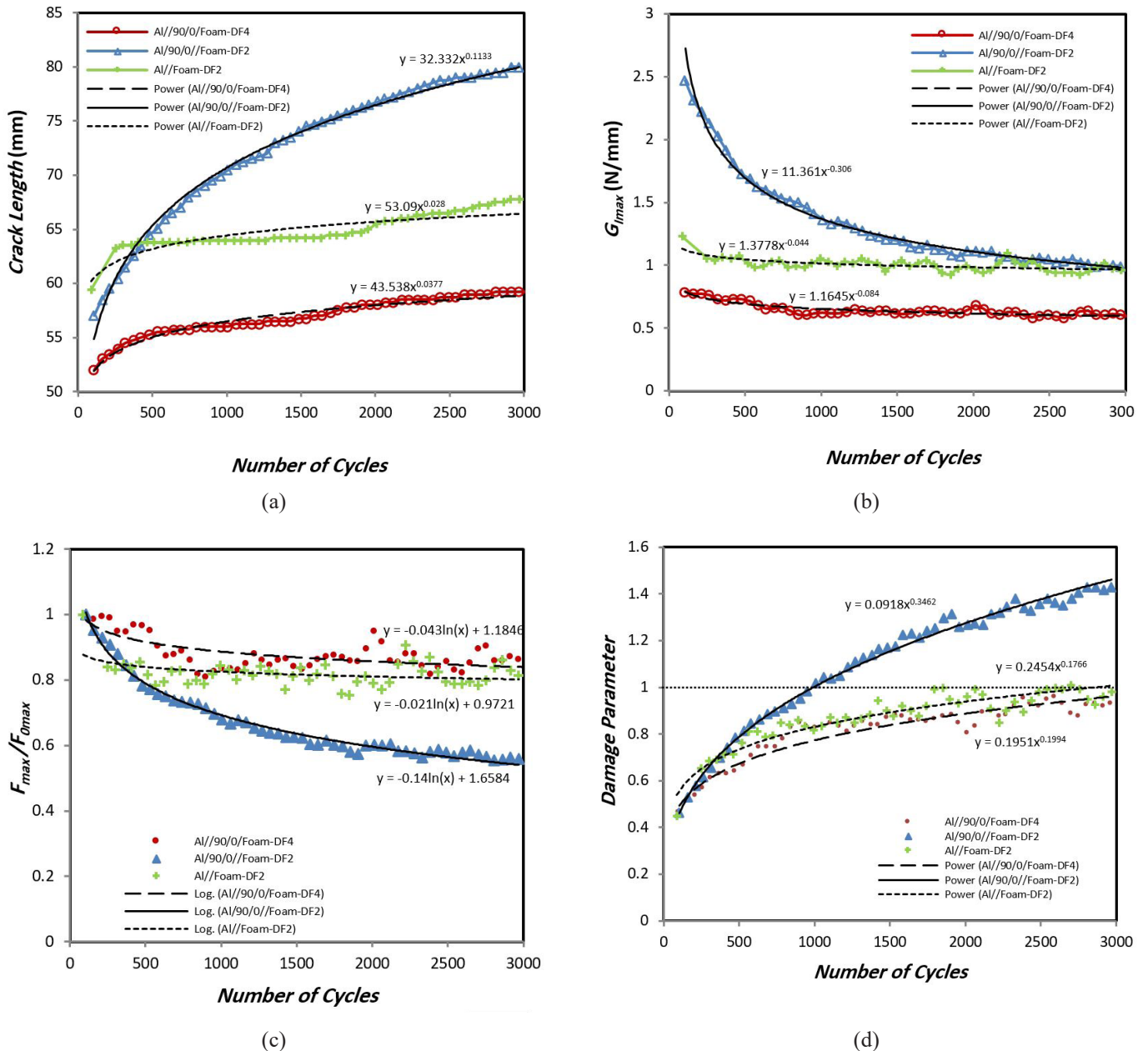


Fig. 10. Mode-I (a) debonding growth versus number of cycles, (b) maximum cyclic strain energy release rate versus number of cycles, (c) load reduction as a function of cycles number, (d) damage evolution according to number of cycles.

number of cycles. The maximum cyclic mode-II strain energy release rate for (Al//90/0//Foam/0/90/Al) sandwich layups is greater than (Al//Foam/Al) layup configurations, hence the fatigue delamination growth rate of (Al//90/0//Foam/0/90/Al) sandwich layup is greater than (Al//Foam/Al) layup configuration. Based on Fig. 13, the total debonding length for (Al//90/0//Foam/0/90/Al) layup configuration is greater than (Al//Foam/Al) layup after 250 cycles.

Figs. 12 (c) and 12 (d) show the load reduction and damage evolution versus the number of cycles for several sandwich layups in mode-II loading condition respectively. Since the strength of aluminum face sheet is lower than FML face sheet in shear loading condition, hence the stiffness reduction of (Al//Foam/Al) sandwich layups is larger than the values for two other layup configurations, subsequently the damage growth of (Al//Foam/Al) layup is faster than those obtained

for (Al//90/0//Foam/0/90/Al) and (Al//90/0//Foam/0/90/Al) layups. Although the stiffness reduction of (Al//90/0//Foam/0/90/Al) layup is larger than (Al//90/0//Foam/0/90/Al) layup, but the damage initiation and propagation of (Al//90/0//Foam/0/90/Al) layup is smaller than (Al//90/0//Foam/0/90/Al) layup. Only foam core failure mode occurred in (Al//90/0//Foam/0/90/Al) layup but combined foam failure and delamination modes occurred in (Al//90/0//Foam/0/90/Al) layup, Hence we observe faster damage growth in (Al//90/0//Foam/0/90/Al) sandwich layup configuration. So, in mode-II fatigue loading the (Al//Foam/Al) sandwich layup is the least efficient layup configuration. Table 7 shows the detailed global damage parameter versus number of cycles for different layups under mode-II fatigue loading. From this table it is understood that (Al//Foam/Al) sandwich beam is the first layup configurations whose global damage parameter

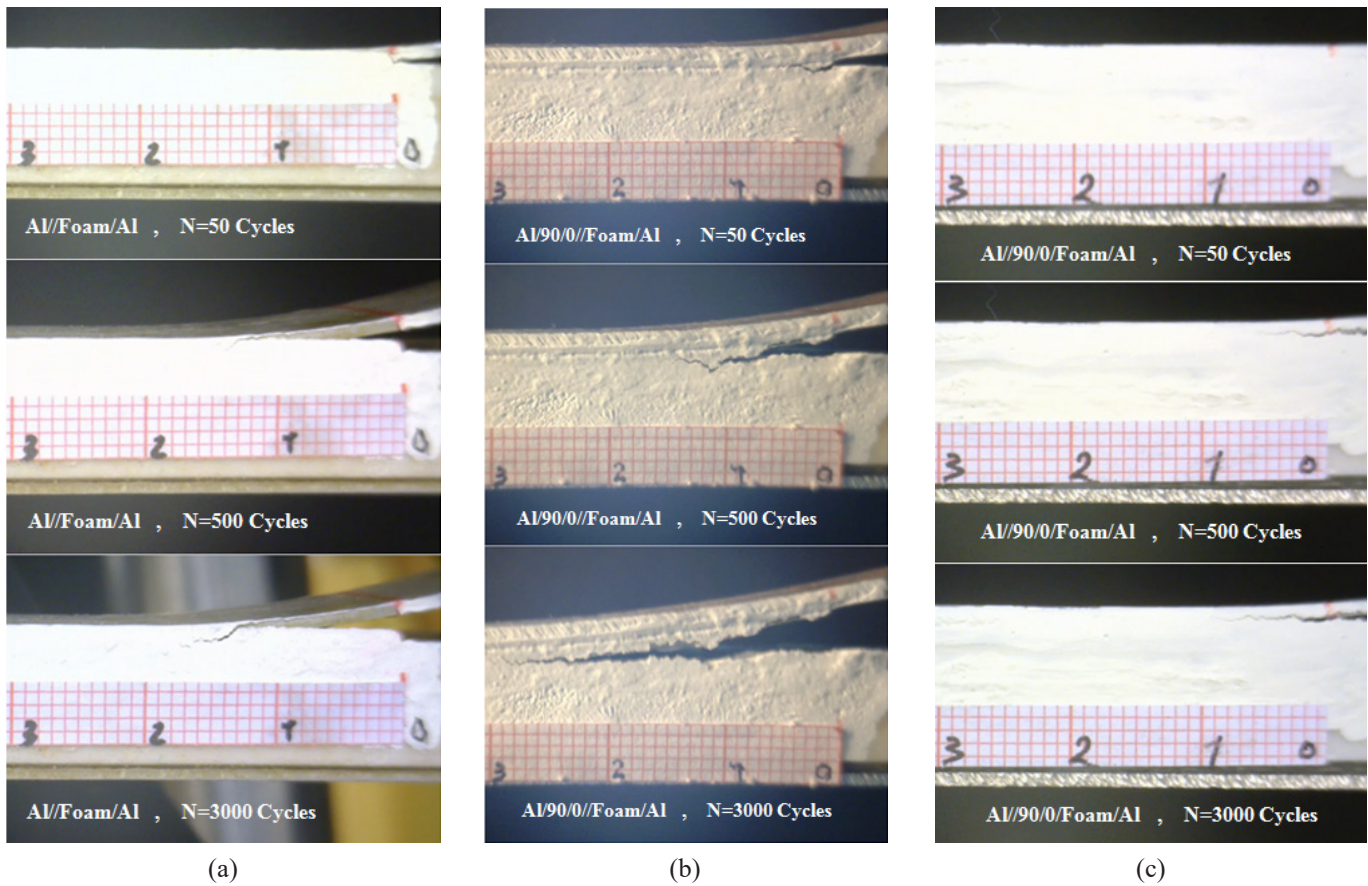


Fig. 11. Mode-I fatigue debonding and crack growth, (a) Al/Foam/Al, (b) Al/90/0//Foam/0/90/Al, (c) Al/90/0/Foam/0/90/Al

Table 7. Global damage parameter for mode-II fatigue loading.

Number of Cycles	Global Damage Parameter		
	Al/90/0//Foam/0/90/Al	Al//Foam/Al	Al/90/0/Foam/0/90/Al
50	0.2466	0.4443	0.1931
100	0.2962	0.5588	0.2325
150	0.3297	0.6390	0.2592
200	0.3558	0.7027	0.2800
250	0.3774	0.7565	0.2972
300	0.3960	0.8035	0.3121
350	0.4125	0.8456	0.3253
400	0.4273	0.8837	0.3371
450	0.4409	0.9188	0.3479
500	0.4533	0.9514	0.3579
550	0.4649	0.9819	0.3671
600	0.4757	1.0105	0.3758

reaches unit value in about 600 cycles and it has the greatest damage growth rate versus number of cycles among the investigated layups.

### 7- Conclusion

This paper presents the experimental investigations to characterize the damage evolution of sandwich structures under static and low cycle fatigue loading conditions. The obtained results are highly affected by the initial delamination

location, the type of sandwich beam's face sheet and mode of loading. Generally, we can summarize the significant results as follows:

- In mode-I static loading the interface between aluminum and composite in (Al//90/0/Foam/0/90/Al) layup has the minimum fracture toughness comparing to the other considered layups. Therefore, it has the smallest resistance against the debonding growth and it is the least efficient layup configuration.

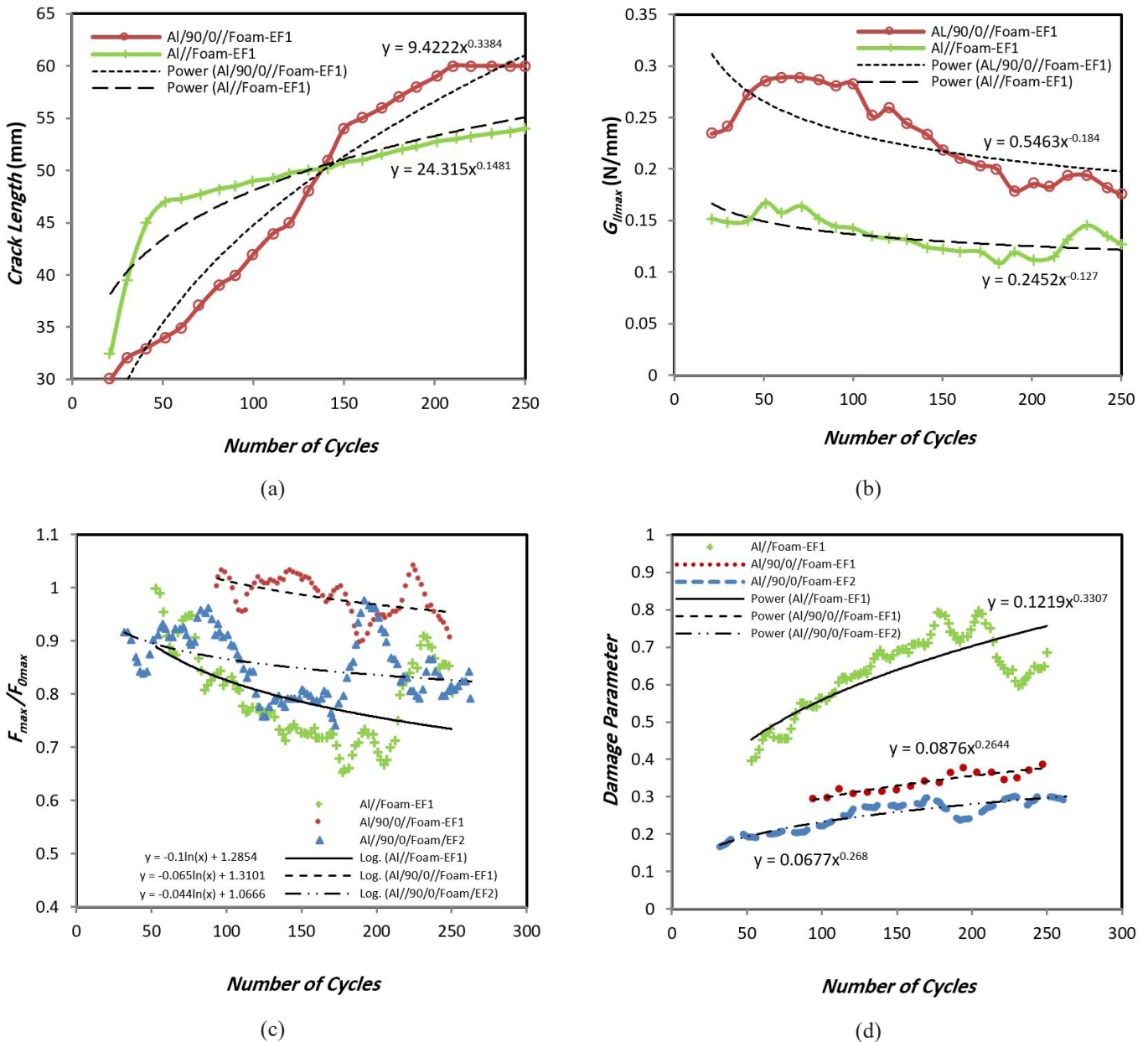


**Fig. 12. Mode-II (a) debonding and crack growth versus number of cycles, (b) maximum cyclic strain energy release rate versus number of cycles, (c) load reduction as a function of number of cycles, (d) damage evolution according to number of cycles.**

- Under mode-II loading condition, shear stress is large enough to initiate and propagate crack in PVC foam core of (Al//90/0//Foam/0/90/Al) layup configuration instead of debonding growth between aluminum and composite. The (Al//Foam/Al) sandwich layup has the most predictable debonding growth under mode-II static loading and it has the most damage accumulation.
- In mode-II static tests, unstable crack growth is present when the load–displacement curve has a semi-vertical tangent. In all other test results in mode-I and mode-II stable crack growth are observed.
- Under mode-I fatigue loading, the debonding growth is very fast at the initial number of cycles. But the debonding growth rate reduces and the crack will remain unchanged near the failure cycles. Since the maximum displacement of (Al//90/0//Foam/0/90/Al) sandwich beam is about half of the other layups. Thus the fatigue debonding growth and damage propagation of this layup is smaller than (Al//Foam/Al) and (Al/90/0//Foam/0/90/Al) layup configurations.
- The fatigue behavior of the sandwich composites in mode-II mainly depends on the progressive developments of different damage mechanisms which also depend on the type of reinforcement, core characteristics, maximum applied loading level and type of loading.
- In mode-II fatigue loading, the (Al//Foam/Al) sandwich layup has the larger stiffness reduction and hence it has the faster damage growth than those obtained for the other layup configurations. So, the (Al//Foam/Al) sandwich layup is the least efficient layup.

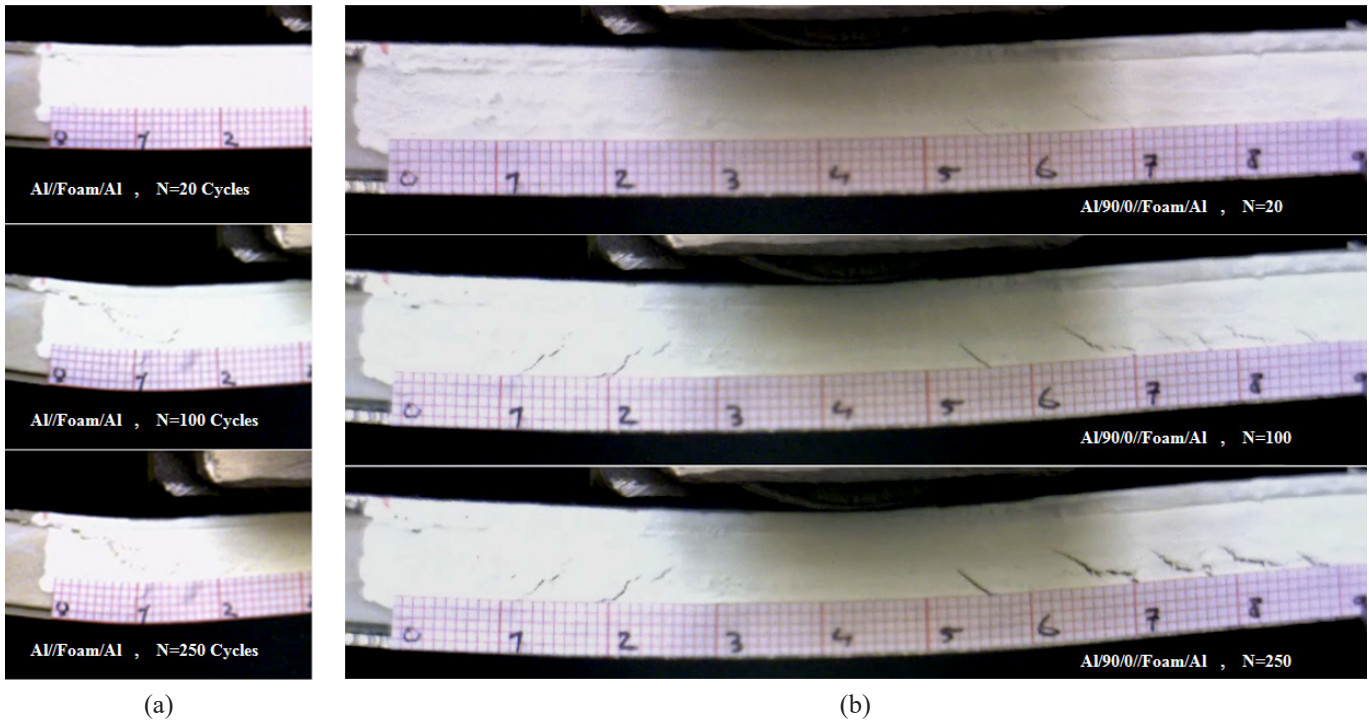


Fig. 13. Mode-II fatigue damage growth, (a) Al/Foam/Al, (b) Al/90/0//Foam/0/90/Al

**Nomenclature**

$E$	Young's modulus, GPa
$E_T$	Tangential Young's modulus, GPa
$G$	Shear modulus, GPa
$A$	Area, N.mm
$W$	Specimen width, mm
$G_{IC}$	Mode-I fracture toughness, N/mm
$G_{IR}$	Mode-I fracture resistance, N/mm
$P$	Load, N
$L$	Specimen span, mm
$a_0$	Initial debonding length, mm
$G_{IIC}$	Mode-II fracture toughness, N/mm
$G_{IIR}$	Mode-II fracture resistance, N/mm
$N$	Number of cycles
$R$	Displacement ratio
$P_{max}$	Maximum cyclic load, N
$G_{I_{max}}$	Maximum cyclic mode-I strain energy release rate, N/mm
$G_{II_{max}}$	Maximum cyclic mode-II strain energy release rate, N/mm
$D$	Global damage parameter

**Greek symbols**

$\nu$	Poisson's ratio
$\sigma_y$	Yield stress, MPa
$\sigma_u$	Ultimate stress, MPa
$\Delta a$	Debonding growth, mm

$\delta$	Displacement, mm
$[\delta_{cr}]_{av}$	Average value of critical load displacement, mm
$\delta_{min}$	Minimum cyclic displacement, mm
$\delta_{max}$	Maximum cyclic displacement, mm

**References**

- [1] J. Rodríguez-González, A. May-Pat, F. Avilés, A beam specimen to measure the face/core fracture toughness of sandwich materials under a tearing loading mode, *International Journal of Mechanical Sciences*, 79 (2014) 84-94.
- [2] A.A. Saaid, S.L. Donaldson, Experimental and finite element evaluations of debonding in composite sandwich structure with core thickness variations, *Advances in Mechanical Engineering*, 8(9) (2016) 1687814016667418.
- [3] A. Nazari, H. Hosseini-Toudeshky, M. Kabir, Experimental investigations on the sandwich composite beams and panels with elastomeric foam core, *Journal of Sandwich Structures & Materials*, (2017) 1099636217701093.
- [4] A. Nazari, M. Kabir, H. Hosseini Toudeshky, Investigation of elastomeric foam response applied as core for composite sandwich beams through progressive failure of the beams, *Journal of Sandwich Structures & Materials*, (2017) 1099636217697496.
- [5] A. Nazari, M. Kabir, H. Hosseini-Toudeshky, Y. Alizadeh Vaghasloo, S. Najafian, Investigation of progressive failure in the composite sandwich panels with elastomeric foam core under concentrated loading, *Journal of Sandwich Structures & Materials*, (2017)

1099636217719424.

- [6] T. Sinmazcelik, E. Avcu, M.Ö. Bora, O. Çoban, A review: Fibre metal laminates, background, bonding types and applied test methods, *Materials & Design*, 32(7) (2011) 3671-3685.
- [7] F. Mazaheri, H. Hosseini-Toudeshky, Low-cycle fatigue delamination initiation and propagation in fibre metal laminates, *Fatigue & Fracture of Engineering Materials & Structures*, 38(6) (2015) 641-660.
- [8] H. Plokker, S. Khan, R. Alderliesten, R. Benedictus, Fatigue crack growth in fibre metal laminates under selective variable-amplitude loading, *Fatigue & Fracture of Engineering Materials & Structures*, 32(3) (2009) 233-248.
- [9] P.-Y. Chang, J.-M. Yang, Modeling of fatigue crack growth in notched fiber metal laminates, *International Journal of Fatigue*, 30(12) (2008) 2165-2174.
- [10] P.Y. Chang, J.M. Yang, H.-s. Seo, H. Hahn, Off-axis fatigue cracking behaviour in notched fibre metal laminates, *Fatigue & Fracture of Engineering Materials & Structures*, 30(12) (2007) 1158-1171.
- [11] H.Z. Jishi, R. Umer, W.J. Cantwell, Skin-core debonding in resin-infused sandwich structures, *Polymer Composites*, 37(10) (2016) 2974-2981.
- [12] G. Martakos, J. Andreasen, C. Berggreen, O. Thomsen, Experimental investigation of interfacial crack arrest in sandwich beams subjected to fatigue loading using a novel crack arresting device, *Journal of Sandwich Structures & Materials*, 0(0) (2017) 1099636217695057.
- [13] Z.T. Kier, A.M. Waas, *Determining Effective Interface Fracture Properties of 3D Fiber Reinforced Foam Core Sandwich Structures*, in: 57th AIAA/ASCE/AHS/ASC Structures, Structural Dynamics, and Materials Conference, American Institute of Aeronautics and Astronautics, 2016.
- [14] A. Patra, N. Mitra, Interface fracture of sandwich composites: Influence of MWCNT sonicated epoxy resin, *Composites Science and Technology*, 101 (2014) 94-101.
- [15] L.A. Carlsson, G.A. Kardomateas, *Structural and failure mechanics of sandwich composites*, Springer Science & Business Media, 2011.
- [16] F. Mazaheri, H. Hosseini-Toudeshky, Experimental Investigations on Fracture Toughness of Sandwich Beams with Foam Core and FML face sheets, in: 11<sup>th</sup> International Conference on Composite Science and Technology, Sharjah, UAE, 2017.
- [17] F. Aviles, L. Carlsson, Analysis of the sandwich DCB specimen for debond characterization, *Engineering Fracture Mechanics*, 75(2) (2008) 153-168.
- [18] Y. Hirose, G. Matsubara, M. Hojo, H. Matsuda, F. Inamura, Evaluation of mode I crack suppression method for foam core sandwich panel with fracture toughness test and analyses, in: Proc. Mechanical Engineering Congress, 2006, pp. 171-172.
- [19] V. Rizov, Mixed-mode I/III fracture study of sandwich beams, *Cogent Engineering*, 2(1) (2015) 993528.
- [20] A. Quispitupa, C. Berggreen, L.A. Carlsson, Face/core interface fracture characterization of mixed mode bending sandwich specimens, *Fatigue & Fracture of Engineering Materials & Structures*, 34(11) (2011) 839-853.
- [21] R. Sheno, S. Clark, H. Allen, Fatigue behaviour of polymer composite sandwich beams, *Journal of Composite Materials*, 29(18) (1995) 2423-2445.
- [22] M. Burman, D. Zenkert, Fatigue of foam core sandwich beams—1: undamaged specimens, *International journal of fatigue*, 19(7) (1997) 551-561.
- [23] N. Kulkarni, H. Mahfuz, S. Jeelani, L.A. Carlsson, Fatigue crack growth and life prediction of foam core sandwich composites under flexural loading, *Composite Structures*, 59(4) (2003) 499-505.
- [24] K. Kanny, H. Mahfuz, Flexural fatigue characteristics of sandwich structures at different loading frequencies, *Composite Structures*, 67(4) (2005) 403-410.
- [25] A. Bezzazi, A. El Mahi, J.-M. Berthelot, B. Bezzazi, Experimental analysis of behavior and damage of sandwich composite materials in three-point bending. Part 1. Static tests and stiffness degradation at failure studies, *Strength of materials*, 39(2) (2007) 170-177.
- [26] D. Zenkert, M. Burman, Failure mode shifts during constant amplitude fatigue loading of GFRP/foam core sandwich beams, *International Journal of Fatigue*, 33(2) (2011) 217-222.
- [27] F. Yang, Q. Lin, J. Jiang, Experimental study on fatigue failure and damage of sandwich structure with PMI foam core, *Fatigue & Fracture of Engineering Materials & Structures*, 38(4) (2015) 456-465.
- [28] M. Burman, D. Zenkert, Fatigue of foam core sandwich beams. II. Effect of initial damage, *International Journal of Fatigue(UK)*, 19(7) (1997) 563-578.
- [29] A. Shipsha, M. Burman, D. Zenkert, Interfacial fatigue crack growth in foam core sandwich structures, *Fatigue & fracture of engineering materials & structures*, 22(2) (1999) 123-131.
- [30] A. Shipsha, M. Burman, D. Zenkert, On mode I fatigue crack growth in foam core materials for sandwich structures, *Journal of Sandwich Structures & Materials*, 2(2) (2000) 103-116.
- [31] A. Quispitupa, C. Berggreen, L.A. Carlsson, Fatigue debond growth in sandwich structures loaded in mixed mode bending (MMB), *ECCM13*.(2008).
- [32] M. Manca, A. Quispitupa, C. Berggreen, L.A. Carlsson, Face/core debond fatigue crack growth characterization using the sandwich mixed mode bending specimen, *Composites Part A: Applied Science and Manufacturing*, 43(11) (2012) 2120-2127.
- [33] G. Tuncol, Modeling the Vacuum Assisted Resin Transfer Molding (VARTM) Process for Fabrication of Fiber/metal Hybrid Laminates, Michigan State University. Mechanical Engineering, 2010.
- [34] M. Baucio, *ASM metals reference book*, ASM international, 1993.
- [35] W.H. Seemann III, *Plastic transfer molding techniques for the production of fiber reinforced plastic structures*, in, Google Patents, 1990.

- [36] W. Seemann, *Unitary vacuum bag for forming fiber reinforced composite articles*, in, Google Patents, 1994.
- [37] B.W. Grimsley, *Characterization of the vacuum assisted resin transfer molding process for fabrication of aerospace composites*, Virginia Tech, 2005.
- [38] E. Baumert, W. Johnson, R. Cano, B. Jensen, E. Weiser, Fatigue damage development in new fibre metal laminates made by the VARTM process, *Fatigue & Fracture of Engineering Materials & Structures*, 34(4) (2011) 240-249.
- [39] D. Lefebvre, B. Ahn, D. Dillard, J. Dillard, The effect of surface treatments on interfacial fatigue crack initiation in aluminum/epoxy bonds, *International journal of fracture*, 114(2) (2002) 191-202.
- [40] Standard Guide for Preparation of Metal Surfaces for Adhesive Bonding, in: Designation D, ASTM, 2001.
- [41] A. Bezazi, A. El Mahi, J.-M. Berthelot, B. Bezzazi, Experimental analysis of behavior and damage of sandwich composite materials in three-point bending. Part 1. Static tests and stiffness degradation at failure studies, *Strength of materials*, 39(2) (2007) 170-177.
- [42] R.C. Østergaard, B.F. Sørensen, P. Brøndsted, Measurement of interface fracture toughness of sandwich structures under mixed mode loadings, *Journal of Sandwich Structures & Materials*, 9(5) (2007) 445-466.
- [43] J. Sinke, H.d. Boer, P. Middendorf, Testing and Modeling of Failure Behavior in Fiber Metal Laminates, in: 25<sup>TH</sup> *International Congress of the Aeronautical Science*, Hamburg, Germany, 2006.
- [44] M.S. Prasad, C. Venkatesha, T. Jayaraju, Experimental methods of determining fracture toughness of fiber reinforced polymer composites under various loading conditions, *Journal of Minerals and Materials Characterization and Engineering*, 10(13) (2011) 1263.
- [45] C. Berggreen, B.C. Simonsen, K.K. Borum, Experimental and numerical study of interface crack propagation in foam-cored sandwich beams, *Journal of composite materials*, 41(4) (2007) 493-520.
- [46] M. Shokrieh, M. Heidari-Rarani, M. Ayatollahi, Delamination R-curve as a material property of unidirectional glass/epoxy composites, *Materials & Design*, 34 (2012) 211-218
- [47] Standard Test Method for Mode I Fatigue Delamination Growth Onset of Unidirectional Fiber-Reinforced Polymer Matrix Composites, in: Designation D., ASTM, 1997.
- [48] O. Al-Khudairi, H. Hadavinia, A. Waggott, E. Lewis, C. Little, Characterising mode I/mode II fatigue delamination growth in unidirectional fibre reinforced polymer laminates, *Materials & Design* (1980-2015), 66 (2015) 93-102.
- [49] A. El Mahi, M.K. Farooq, S. Sahraoui, A. Bezazi, Modelling the flexural behaviour of sandwich composite materials under cyclic fatigue, *Materials & design*, 25(3) (2004) 199-208.

Please cite this article using:

F. Mazaheri and H. Hosseini-Toudeshky, Experimental Investigations of Static and Fatigue Crack Growth in Sandwich Structures with Foam Core and Fiber-Metal Laminates Face Sheets, *AUT J. Mech. Eng.*, 2(2) (2018) 149-164.

DOI: 10.22060/ajme.2018.14222.5714



